

Trajectory assessment and optimisation in the context of small launcher design

Alexandru-Iulian ONEL^{*,1,2}, Teodor-Viorel CHELARU²

*Corresponding author

^{*,1}INCAS – National Institute for Aerospace Research “Elie Carafoli”,
B-dul Iuliu Maniu 220, 061126, Bucharest, Romania,
onel.alexandru@incas.ro

²“POLITEHNICA” University of Bucharest, Faculty of Aerospace Engineering,
Str. Gheorghe Polizu 1-7, 011061, Bucharest, Romania,
teodor.chelaru@upb.ro

DOI: 10.13111/2066-8201.2020.12.2.10

Received: 26 February 2020/ Accepted: 31 March 2020/ Published: June 2020

Copyright © 2020. Published by INCAS. This is an “open access” article under the CC BY-NC-ND license (<http://creativecommons.org/licenses/by-nc-nd/4.0/>)

Abstract: *The paper presents a mathematical model that can be used to quickly define a nominal trajectory for the studied small launcher configuration. The tool developed based on the proposed mathematical model can be used separately for trajectory assessments or it can be integrated in a multidisciplinary optimisation algorithm for a preliminary small launcher design, together with the trajectory optimisation for a maximum orbital performance.*

Key Words: *mathematical model, trajectory assessment, small launcher, multidisciplinary optimisation, orbital performance*

1. INTRODUCTION

Small dedicated launchers have increased in popularity in the last years because of their operational flexibility towards the consumers’ orbital request. The launcher nominal mission can be now defined by the small cargo (mini or micro satellites) rather than by the medium/large satellites (piggyback missions).

In the small launcher optimisation context, the efficient way to ensure an overall competitive launcher is by using a multidisciplinary design optimisation (MDO) approach. The current paper continues the work previously elaborated in [1], [2], [3] by using the same MDO tool architecture, as seen in Figure 1.

The developed MDO tool employs four main disciplines that are assessed in a cascade order: Weights and Sizing, Propulsion, Aerodynamics and Trajectory together with secondary modules (Inputs, Optimisation variables, Objection function). In this paper a mathematical model that can be used for a quick trajectory assessment and optimisation is presented. As detailed in [1], MDO solution convergence can occur after hundreds of thousands iterations; therefore it is of great interest to reduce the complexity of the used mathematical models. The main approach in reducing MDO complexity is to use a 3DOF dynamic model. Several 3DOF problem formulations can be used ([4], [5], [6]), this paper employing a null bank angle model.

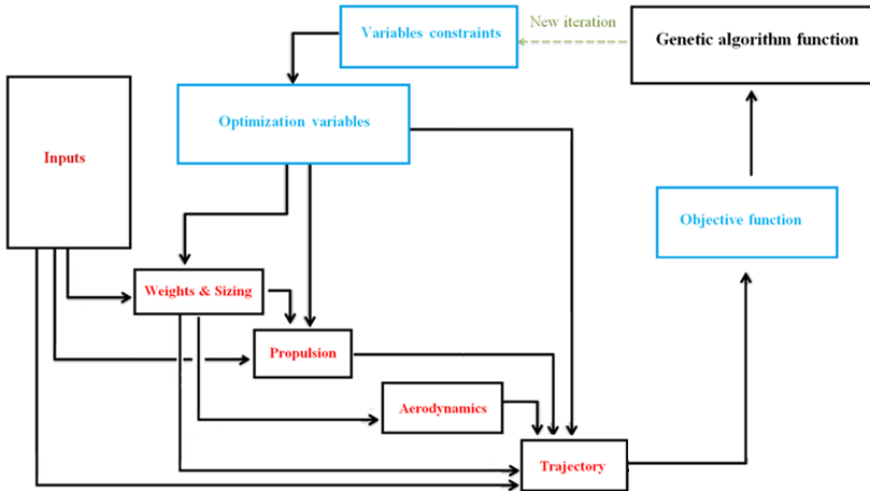


Figure 1 – Block scheme of small launcher MDO tool [1], [2], [3]

In the Trajectory module the main objective is to integrate the equation of motion to accurately simulate the dynamic behaviour of the launcher during its flight. In the small launcher optimisation context, the objective expands and also includes the definition of a nominal optimal trajectory that maximizes imposed criteria (such as maximizing orbital performance).

2. TRAJECTORY ASSESMENT

The problem of inserting a satellite into the desired orbit is a difficult one to solve. If the launcher's trajectory is not well computed, it can lead to an unsuccessful deployment of the payload into its desired orbit but also to flight emergency interruption. This is why it is of great importance to use a dynamic model with a high results accuracy, together with a correct formulation of the problem of the small launcher flight.

The equations of motion are written in the quasi-velocity frame because of their simplicity in numerical implementation. The quasi-velocity frame has the origin in the launcher centre of mass, and participates in the diurnal rotation. The x axis is along the velocity vector, the y axis is up in vertical plane and the z axis completes the right trihedral. Detailed presentation of the coordinate systems specific to the motion of launch systems is shown in [7] and [8].

The 3DOF dynamic equations which describe the centre of mass motion in the quasi-velocity frame are ([7], [9]):

$$\begin{aligned} \dot{V} &= \frac{N_x}{m} - g_r \sin \gamma - g_\omega (\cos \varphi \cos \chi \cos \gamma + \sin \varphi \sin \gamma) \\ \dot{\gamma} &= \frac{N_y}{mV} - \frac{g_r}{V} \cos \gamma - \frac{g_\omega}{V} (-\cos \varphi \cos \chi \sin \gamma + \sin \varphi \cos \gamma) + \frac{V}{r} \cos \gamma - 2\Omega_p \cos \varphi \sin \chi \\ \dot{\chi} &= -\frac{N_z}{mV \cos \gamma} + \frac{g_\omega \cos \varphi \sin \chi}{V \cos \gamma} + \frac{V}{r} \tan \varphi \sin \chi \cos \gamma + 2\Omega_p (\cos \varphi \cos \chi \tan \gamma - \sin \varphi) \end{aligned} \quad (1)$$

The kinematic equations which complete the 3DOF system are ([10], [12]):

$$\dot{\varphi} = \frac{V}{r} \cos \chi \cos \gamma, \dot{\lambda} = -\frac{V \sin \chi \cos \gamma}{r \cos \varphi}, \dot{r} = V \sin \gamma \quad (2)$$

where: V is the launcher velocity, γ is the climb angle, χ is the path track angle, φ is the geocentric latitude, λ is the relative geocentric longitude, r is the centre of mass – centre of Earth distance, N_x, N_y, N_z are the projection of the applied forces along the quasi-velocity frame, m is the launcher mass, g_r and g_ω are the gravitational acceleration radial and polar components, Ω_p is the Earth angular velocity.

The equations presented in (2) describe the evolution of the position vector \vec{r} , while the equations presented in (1) describe the evolution of the velocity vector \vec{v} .

The employed gravitation model is the J2 model [7], where the gravitational acceleration (attraction and centrifugal components), is expressed by two terms, one along radius r (g_r) and the second parallel to the polar axis N-S (g_ω). The following relations are implemented in the model:

$$\begin{aligned} g_r &= \frac{a_{00}}{r^2} - \frac{3}{2} \frac{a_{20}}{r^4} (5 \sin^2 \varphi - 1) - \Omega_p^2 r \dots \\ g_\omega &= 3 \frac{a_{20}}{r^4} \sin \varphi + \Omega_p^2 r \sin \varphi \dots \end{aligned} \quad (3)$$

with:

$$\begin{aligned} a_{00} &= 3.9861679 \cdot 10^{14} \\ \frac{3}{2} a_{20} &= 26.32785 \cdot 10^{24} \end{aligned} \quad (4)$$

The projection of the applied forces along the quasi-velocity frame N_x, N_y, N_z are computed using:

$$N_{quasi-velocity} = \begin{bmatrix} N_x \\ N_y \\ N_z \end{bmatrix} = B_{\mu\beta^*\alpha} \cdot \left(\begin{bmatrix} X^T \\ Y^T \\ Z^T \end{bmatrix} + \begin{bmatrix} X^F \\ Y^F \\ Z^F \end{bmatrix} \right) \Big|_{body} \quad (5)$$

where T corresponds to propulsive forces and F corresponds to aerodynamic forces.

Because it is easier to write the applied forces components in the body frame, the rotation matrix $B_{\mu\beta^*\alpha}$ is used to transfer data between the body and quasi-velocity frames.

$$B_{\mu\beta^*\alpha} = \begin{bmatrix} \cos \alpha \cos \beta^* & -\sin \alpha \cos \beta^* & \sin \beta^* \\ \sin \alpha \cos \mu + \cos \alpha \sin \beta^* \sin \mu & \cos \alpha \cos \mu - \sin \alpha \sin \beta^* \sin \mu & -\cos \beta^* \sin \mu \\ \sin \alpha \sin \mu - \cos \alpha \sin \beta^* \cos \mu & \cos \alpha \sin \mu + \sin \alpha \sin \beta^* \cos \mu & \cos \beta^* \cos \mu \end{bmatrix} \quad (6)$$

For this paper a null bank angle 3DOF model is used, which corresponds with the following assumption:

- The control sequence in the GNC system ensures that the thrust vector is aligned with the body axis;
- Between the launcher and the velocity vector two non-zero aerodynamic angles exist: $\alpha \neq 0, \beta^* \neq 0$;
- The bank angle is null $\mu = 0$.

The applied forces can be seen in Figure 2. Due to the assumptions of the implemented dynamic model, the projection of the propulsive force along the body frame is defined by:

$$T_{body} = \begin{bmatrix} X^T \\ Y^T \\ Z^T \end{bmatrix} = \begin{bmatrix} T \\ 0 \\ 0 \end{bmatrix} \quad (7)$$

with T being the propulsion force.

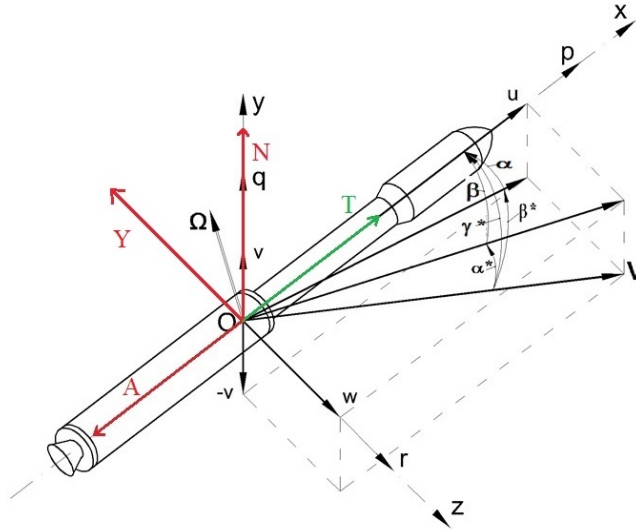


Figure 2 – Body frame and applied forces

The projection of the aerodynamic force along the body frame is defined by:

$$F_{body} = \begin{bmatrix} X^F \\ Y^F \\ Z^F \end{bmatrix} = \begin{bmatrix} -A \\ N \\ -Y \end{bmatrix} = \begin{bmatrix} -q \cdot S_{ref} \cdot C_A \\ q \cdot S_{ref} \cdot C_N \\ -q \cdot S_{ref} \cdot C_Y \end{bmatrix} \quad (8)$$

where: A is the axial force, N is the normal force, Y is the side force.

The aerodynamic characteristics of the studied launcher are analysed in the Aerodynamic module of the MDO tool. For this paper, the mathematical models described in [2] and [13] are used. The active control of the launcher is realised by orienting the thrust vector with respect to the velocity vector. Because of the model assumptions, the orientation of the launcher can be modified if one considers the aerodynamic angles α and β^* as being command parameters of the system. With these command parameters the climb angle and path track angle (cinematic azimuth) can be controlled based on feedback control loops such as:

$$\begin{aligned} \alpha &= -k_1(\gamma - \gamma_d) \\ \beta^* &= -k_1(\chi - \chi_d) \end{aligned} \quad (9)$$

where reference sizes are γ_d and χ_d .

In order to carry out a correct analysis of the trajectory-specific orbital performances obtained by integrating the differential system of 6 equations corresponding to the 3DOF model used, it is necessary to convert the position vector \vec{r} and the velocity vector \vec{v} into the classical orbital parameters of $a, e, i, \Omega, \omega, f$ (semi major axis, eccentricity, inclination, longitude of the ascending node, argument of perigee and true anomaly). The first two parameters define the trajectory of the studied body in the orbital plane, the next three define the orientation of the orbital plane in space, while the latter defines the position of the body on the orbit.

First, the position and velocity vectors obtained in the quasi-velocity frame must be transposed in an inertial frame, the most used being ECI (Earth Centred Inertial).

As detailed in [8], the position vector in ECI is described by:

$$\begin{aligned} X_{ECI} &= r \cos \varphi \cos \lambda_a \\ Y_{ECI} &= r \cos \varphi \sin \lambda_a \\ Z_{ECI} &= r \sin \varphi \end{aligned} \quad (10)$$

with the absolute geocentric longitude $\lambda_a = \lambda + \Omega_p t$.

Also, from [8], the velocity in ECI is described by:

$$\begin{bmatrix} V_{x_{ECI}} \\ V_{y_{ECI}} \\ V_{z_{ECI}} \end{bmatrix} = B_G \cdot \begin{bmatrix} V \cos \gamma \cos \chi \\ V \sin \gamma \\ -V \cos \gamma \sin \chi + r \Omega_p \cos \varphi \end{bmatrix} \quad (11)$$

with the rotation matrix:

$$B_G = \begin{bmatrix} -\sin \varphi \cos \lambda_a & \cos \varphi \cos \lambda_a & -\sin \lambda_a \\ -\sin \varphi \sin \lambda_a & \cos \varphi \sin \lambda_a & \cos \lambda_a \\ \cos \varphi & \sin \varphi & 0 \end{bmatrix} \quad (12)$$

Now that the position vector \vec{r} and the velocity vector \vec{v} are obtained in ECI frame, we can obtain the six orbital parameters, based on the work done in [11]. First, the angular momentum vector \vec{h} , the node vector \vec{n} and the eccentricity vector \vec{e} are computed:

$$\begin{aligned} \vec{h} &= \vec{r} \times \vec{v} \\ \vec{n} &= \begin{bmatrix} 0 \\ 0 \\ 1 \end{bmatrix} \times \vec{h} \\ \vec{e} &= \frac{1}{\mu} \vec{v} \times \vec{h} - \frac{\vec{r}}{r} \end{aligned} \quad (13)$$

with μ being the standard gravitational parameter.

The following scalars are now computed (including eccentricity):

$$r = \|\vec{r}\|, \quad v = \|\vec{v}\|, \quad e = \|\vec{e}\|, \quad h = \|\vec{h}\|, \quad n = \|\vec{n}\| \quad (14)$$

The semi major axis is obtained from:

$$a = -\frac{\mu}{2E}, \quad E = \frac{v^2}{2} - \frac{\mu}{r} \quad (15)$$

The inclination is now computed:

$$i = \cos^{-1} \left(\frac{\vec{h}}{h} \cdot \begin{bmatrix} 0 \\ 0 \\ 1 \end{bmatrix} \right) \quad (16)$$

The longitude of the ascending node is obtained from:

$$\Omega = \cos^{-1} \left(\begin{bmatrix} 0 \\ 0 \\ 1 \end{bmatrix} \cdot \frac{\vec{n}}{n} \right) \quad (17)$$

with the following quadrant correction ($\hat{y} = [0 \ 1 \ 0]$):

$$\Omega = \begin{cases} \Omega, & \text{if } \hat{y} \cdot \vec{n} \geq 0 \\ 360^\circ - \Omega, & \text{if } \hat{y} \cdot \vec{n} < 0 \end{cases} \quad (18)$$

The argument of perigee is obtained from:

$$\omega = \cos^{-1} \left(\frac{\vec{n} \cdot \vec{e}}{n \cdot e} \right) \quad (19)$$

with the following quadrant correction ($\hat{z} = [0 \ 0 \ 1]$):

$$\omega = \begin{cases} \omega, & \text{if } \hat{z} \cdot \vec{e} \geq 0 \\ 360^\circ - \omega, & \text{if } \hat{z} \cdot \vec{e} < 0 \end{cases} \quad (20)$$

Finally, the true anomaly can be computed:

$$f = \cos^{-1} \left(\frac{\vec{r} \cdot \vec{e}}{r \cdot e} \right) \quad (21)$$

with the following quadrant correction:

$$f = \begin{cases} f, & \text{if } \vec{r} \cdot \vec{v} \geq 0 \\ 360^\circ - f, & \text{if } \vec{r} \cdot \vec{v} < 0 \end{cases} \quad (22)$$

3. FLIGHT PHASES

For small launchers, it is preferable to use a direct trajectory (DATO - Direct ascent to orbit), this being the simplest method of inserting a satellite into Low Earth Orbit. Even though the payload mass is lower than for a two-burn trajectory, the DATO is a preferred strategy, because the complexity of rocket engines is lower, no successive stops and restarts required. Furthermore, the time required for the launcher to accomplish its mission is minimal, thus reducing the occurrence of any eventual risks.

To define the launcher mission, several flight phases occur, which have impact on the system of equations or control definition numerical implementation. For simplicity and also correlation with studied configuration a two-stage launcher DATO mission will be detailed and its flight phases presented. Thus, the following flight phases occur for a two-stage small launcher aiming a DATO mission, as seen in Figure 3:

- (a) *Vertical flight*: corresponds to the period immediately after launch, period in which the axis of symmetry of the launcher is aligned with the velocity vector. The aerodynamic angles α and β^* are zero. The climb angle γ is 90° .
- (b) *First stage active guidance*: the climb angle γ is reduced towards a target value γ_{d1} and kept it constant for a short period (to align the velocity vector with that of the thrust/body of the launcher). If the imposed launch direction does not allow the satellite to be placed in an orbit of a certain inclination, then a path track angle χ_{d1} is also required. The aerodynamic angles α and β^* can be non-zero.
- (c) *First stage gravitational turn*: is characterized by a lack of normal direction applied forces components, the normal load factor being zero. The climb angle naturally decreases due to gravitational acceleration. The aerodynamic angles α and β^* are zero.
- (d) *First stage separation*: after fuel burnout, the stage is separated to decrease the launcher mass.
- (e) *Fairing jettison*: the fairing is separated from the launch vehicle when one or more separation conditions imposed prior to launch (e.g. Altitude > 50km, Dynamic

pressure < 0.5 kPa, Thermal flux < 1.135 kW/m²) are satisfied. For good controllability, fairing jettison is preferable when the rocket engines are not running.

- (f) *Second stage ignition*: is performed after a coasting phase, period in which the launcher loses kinetic energy (velocity), but gains potential energy (altitude).
- (g) *Second stage gravitational turn*: the movement with natural control (null aerodynamic angles) is continued, the thrust force now being generated by the second stage engine.
- (h) *Second stage active guidance - orbital insertion*: corresponds to the end of the powered flight, finalized by detaching and inserting the payload into the desired orbit. The climb angle of the trajectory approaches the second imposed value γ_{d2} , the path track angle approaches χ_{d2} and the aerodynamic angles α and β^* are non-zero. The aerodynamic effects are very small due to the high altitude at which the launcher is located.

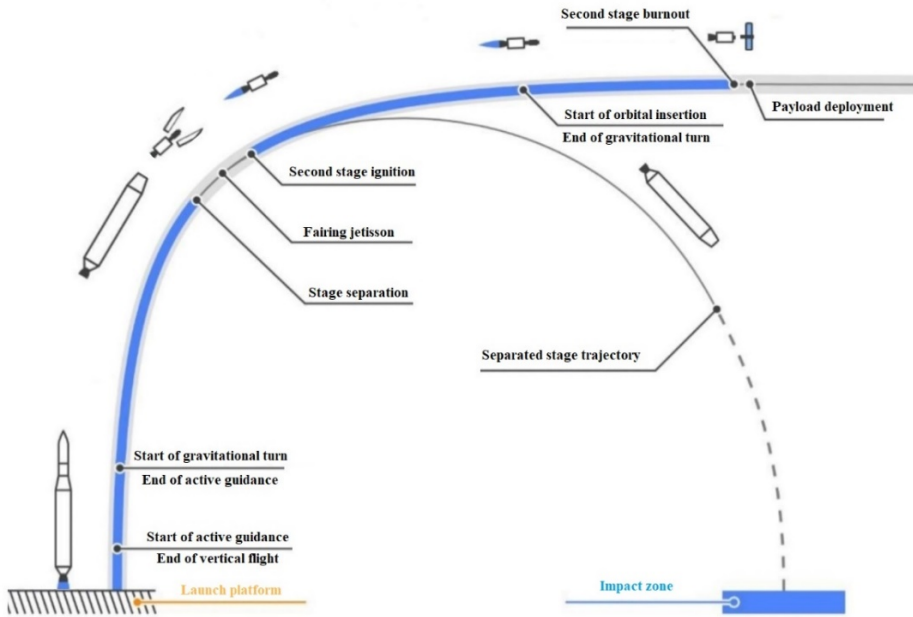


Figure 3 – DATO mission flight phases (two-stage small launcher)

4. TRAJECTORY OPTIMISATION

As for any optimisation problem, the criteria which will be used to select good over bad trajectories must be clearly mathematically defined. For the current case, when discussing the optimisation of a nominal trajectory, the launcher configuration will be considered frozen, input data being obtained from reference documents.

The objective is to obtain the maximum payload mass that can be inserted into a predefined orbit. In addition, any kind of constraint applied to the trajectory (load factors, failure to reach the target parameters and others) must be respected. Iteratively, the objective function will converge to its minimum value (or maximum, depending on how it is defined).

The following objective function is proposed to be minimised:

$$f_{objective} = \left(\frac{m_{reference}}{m_{payload}} + I_{orbit} \right) \cdot I_{constraints} \quad (23)$$

where: $m_{reference}$ is obtained from launcher user manual (if not available, a value of 1 can be used), $m_{payload}$ is the payload mass subject to maximisation, I_{orbit} is the orbit performance index, $I_{constraints}$ is the constraints index.

The orbit performance index is used to quantify the quality of the payload-inserted orbit compared to that imposed prior to launch.

Thus, it is of interest to introduce the orbital parameters previously presented in the mathematical formula. For a circular orbit of altitude H_d and inclination i_d , the following formula is used for the orbit performance index:

$$I_{orbit} = \sqrt{w_a(a - a_d)^2 + w_V(V - V_d)^2 + w_\gamma(\gamma - \gamma_d)^2 + w_i(i - i_d)^2} \quad (24)$$

with: $w_a = 1$, $w_V = 1$, $w_\gamma = 10$, $w_i = 10$ parameter weights.

The target semi major axis is computed with:

$$a_d = R_P + H_d \quad (25)$$

where $R_P = 6378137m$.

The target velocity, for a circular orbit, is computed with:

$$V_d = \sqrt{\frac{\mu}{r_d}} = \sqrt{\frac{\mu}{a_d}} \quad (26)$$

Finally, $\gamma_d = 0$ for a circular orbit. The desired eccentricity $e_d = 0$ was replaced with V_d and γ_d , for a better convergence of the solution ([1], [5]).

The parameters a, V, γ, i are obtained following the integration of the proposed dynamic model, using the data from the moment of payload deployment, at the end of the second stage burn. For ideal insertion $I_{orbit} = 0$.

The constraints index is used to quantify the validity of the obtained trajectory in relation to the imposed requirements. The following formula is proposed:

$$I_{constraints} = \prod_{i=1}^{N_{constraints}} I_{c_i} \quad (27)$$

where: $N_{constraints}$ is the number of imposed constraints, I_{c_i} is the index for the i constraint.

If the constraint is not respected, the term associated with this constraint I_{c_i} would take over unity values, which would increase the objective function. If the constraint is respected then $I_{c_i} = 1$.

Typical constraints include, but are not limited to: maximum axial and normal load factors, maximum heat flux, maximum deviation from imposed control parameters, maximum aerodynamic angles.

The optimisation variables are those data used by the genetic algorithm function to advance the solution of the MDO iterative process, based on an objective function ranking system.

For the current case, when optimising a nominal trajectory for a known launcher, based on the dynamic model detailed in trajectory assessment chapter, the number of optimisation variables that are needed to be used is presented in Table 1.

Table 1 – Optimisation variables needed for n -stage launcher

| Type of optimisation variable | Number of optimisation variables | Total number of optimisation variables |
|-------------------------------|----------------------------------|--|
| $t_{vertical}$ | 1 | 4n + 1 |
| t_{coast} | $n - 1$ | |
| $m_{payload}$ | 1 | |
| γ_d | n | |
| χ_d | n | |
| Δt | n | |

For a two-stage small launcher, a total of 9 optimisation variables are needed: 1 vertical time, 1 coast time, 1 payload mass, 2 desired climb angles and 2 desired path track angles at the end of the active guidance phases, 2 ratios between active guidance and total stage burn time (Δt).

5. TEST CASES

To validate the mathematical model for the trajectory assessment, together with the proposed associated control scheme and optimisation technique, the Falcon 1 small launcher developed by SpaceX will be analysed. Reference data will be taken from [14](User Manual), [15] and [16]. Based on the mathematical models presented in this paper a Matlab tool has been developed. The minimization the objective function detailed in equation (23) is desired, which is equivalent to maximizing the payload mass that can be inserted in a predefined orbit. For the equations of motion integration an adaptive method of Runge-Kutta type will be used, in which the time step is automatically selected according to the integration error.

The input data for the Falcon 1 launcher are shown in Table 2, together with a graphical representation in Figure 4.

Table 2 – Falcon 1 input data [14], [15]

| Input | Stage I | Stage II | Fairing | Launcher |
|----------------------|-----------------------|-------------------|---------|----------|
| Length [m] | 15 | 2.7 | 3.63 | 21.33 |
| Diameter [m] | 1.67 | 1.67 | 1.52 | 1.67 |
| Dry mass [kg] | 1360.77 | 544.31 | 145.14 | 2050.22 |
| Propellant [kg] | 21491.20 | 4036.97 | - | 25528.17 |
| Total mass [kg] | 22851.98 | 4581.28 | - | 27578.4 |
| Engine type | 1 x Merlin 1C | 1 x Kestrel 2 | - | - |
| Thrust [kN] | 346.96 kN (sea level) | 30.69 kN (vacuum) | - | - |
| Specific impulse [s] | 300 (vacuum) | 317 (vacuum) | - | - |
| Burn time [s] | 169 | 418 | - | 587 |



Figure 4 – Falcon 1 geometry [16]

The Falcon 1 payload vs altitude performance for DATO missions will be subject to analysis, circular orbits of 9.1° inclination and altitudes between 200 km and 600 km being investigated.

The reference data from [14] are extracted with the aid of a plot digitizer tool [19] and shown in Table 3.

Table 3 – Falcon 1 payload vs. altitude reference data [14], $i = 9.1^\circ$

| Altitude | Reference payload mass |
|----------|------------------------|
| 200 km | 414 kg |
| 300 km | 370 kg |
| 400 km | 300 kg |
| 500 km | 221 kg |
| 600 km | 130 kg |

The launch location is SpaceX platform in Omelek Island ($\varphi_{initial} = 9.04771$, $\lambda_{initial} = 167.74299$), launch direction is Eastward ($\chi_{initial} = -90^\circ$). The fairing jettison condition is $\dot{q}_{fairing} < 1135 \frac{W}{m^2}$. Heat flux is computed based on analytic expression detailed in [17] and [18].

Other initial conditions used are: $H_{initial} = 0 m$, $\gamma_{initial} = 90^\circ$, $V_{initial} = 1 \frac{m}{s}$. The maximum load factors, from [14] are: $n_{axial} < 7.7$, $n_{normal} < 0.75$. For the feedback control loop parameter from equation (9) a value of $k_1 = 7$ will be used. The following constraints have been used for the aerodynamic angles: $-7^\circ \leq \alpha \leq 7^\circ$, $-7^\circ \leq \beta^* \leq 7^\circ$. For low altitude orbits, $H \leq 300 km$, only in the orbital injection phase, the limits will be extended to $\alpha \leq 14^\circ$ for better insertion accuracy.

The aerodynamic impact is low because the dynamic pressure and the aerodynamic forces have values very close to 0.

The search interval for optimisation variables shown in Table 4 has been implemented in the tool developed. Because of the clear launch direction, no path track angle control is needed for the first stage active guidance phase.

Table 4 – Search interval for optimisation variables

| Lower bound | Optimisation variable | Upper bound | Unit |
|----------------------------|-----------------------|----------------------------|------|
| 0 | $t_{vertical}$ | 100 | [s] |
| 0 | t_{coast} | 100 | [s] |
| $0.75 \cdot m_{reference}$ | $m_{payload}$ | $1.25 \cdot m_{reference}$ | [kg] |
| 50 | γ_{d1} | 85 | [°] |
| -1 | γ_{d2} | 1 | [°] |
| - | χ_{d1} | - | [°] |
| $\chi_{initial} - 5$ | χ_{d2} | $\chi_{initial} + 5$ | [°] |
| 0 | Δt_1 | 0.5 | [-] |
| 0 | Δt_2 | 0.5 | [-] |

6. RESULTS

Following the optimization process for the Falcon 1 launcher nominal trajectories, the following values, presented in Table 5, were obtained for the optimization variables used.

Table 5 – Results, optimisation variables

| Optimisation variable | Optimal value | | | | |
|-----------------------|---------------|----------|----------|----------|----------|
| | H=200 km | H=300 km | H=400 km | H=500 km | H=600 km |
| $t_{vertical}$ [s] | 33.5053 | 40.0359 | 48.3401 | 46.8796 | 47.0148 |
| t_{coast} [s] | 8.3439 | 13.5917 | 26.0342 | 59.4350 | 77.5048 |
| $m_{payload}$ [kg] | 455.4528 | 388.7862 | 319.7552 | 214.0494 | 126.2177 |
| γ_{d_1} [°] | 67.3517 | 60.1784 | 70.2436 | 76.2830 | 73.2213 |
| γ_{d_2} [°] | 0.8333 | 0.7114 | 0.4887 | 0.3764 | 0.0727 |
| χ_{d_1} [°] | - | - | - | - | - |
| χ_{d_2} [°] | -93.5161 | -93.5621 | -93.3435 | -93.2957 | -93.1885 |
| Δt_1 | 0.3105 | 0.4530 | 0.2186 | 0.1802 | 0.3264 |
| Δt_2 | 0.4937 | 0.4842 | 0.2290 | 0.2499 | 0.2836 |

Table 6 presents the duration of key flight phases, deduced based on the optimisation variables from Table 5.

Table 6 – Results, flight phases

| Flight phase | Duration [s] | | | | |
|---------------------------------------|--------------|----------|----------|----------|----------|
| | H=200 km | H=300 km | H=400 km | H=500 km | H=600 km |
| Vertical flight | 33.51 | 40.04 | 48.34 | 46.88 | 47.01 |
| 1 st stage active guidance | 42.07 | 58.42 | 26.38 | 22 | 39.82 |
| 1 st stage gravity turn | 93.43 | 70.55 | 94.28 | 100.12 | 82.17 |
| Coasting | 8.34 | 13.59 | 26.03 | 59.43 | 77.5 |
| 2 nd stage gravity turn | 211.63 | 215.61 | 322.29 | 313.54 | 299.45 |
| Orbital insertion | 206.37 | 202.39 | 95.71 | 104.46 | 118.55 |
| Total mission time | 595.34 | 600.59 | 613.03 | 646.43 | 664.5 |

From the results shown above, we can observe a tendency to increase the duration of the vertical flight and the coasting times with altitude. Increasing the duration of these phases is necessary to reach a higher altitude. At the same time, the need for longer active guidance phases (1st and 2nd stages) can be observed for lower altitudes circular orbits. Typical mission duration is of 10-11 minutes.

To check the orbital insertion accuracy, it is necessary to present the values associated with the I_{orbit} performance index. According to equation (24), we have a total of 4 terms that appear explicitly in the expression of this performance index. The 4 orbital insertion errors are

numerically presented in Table 7. Very good insertions can be observed for high altitude orbits, the insertion errors being slightly increased for the 200km altitude orbit, still maintaining within reasonable limits.

Table 7 – Results, orbital insertion errors

| Target parameter | Insertion error | | | | |
|----------------------------|--------------------------|--------------------------|-------------------------|-------------------------|--------------------------|
| | H=200 km | H=300 km | H=400 km | H=500 km | H=600 km |
| Semimajor axis a_d | $4 \cdot 10^{-1}$ [km] | $2 \cdot 10^{-3}$ [km] | $-3 \cdot 10^{-5}$ [km] | $-2 \cdot 10^{-4}$ [km] | $4 \cdot 10^{-5}$ [km] |
| Inertial velocity V_d | $-7 \cdot 10^{-1}$ [m/s] | $-2 \cdot 10^{-3}$ [m/s] | $2 \cdot 10^{-5}$ [m/s] | $1 \cdot 10^{-4}$ [m/s] | $-4 \cdot 10^{-5}$ [m/s] |
| Climb angle γ_d | $-6 \cdot 10^{-1}$ [°] | $-8 \cdot 10^{-4}$ [°] | $5 \cdot 10^{-5}$ [°] | $1 \cdot 10^{-5}$ [°] | $-4 \cdot 10^{-7}$ [°] |
| Inclination i_d | $-5 \cdot 10^{-2}$ [°] | $-1 \cdot 10^{-2}$ [°] | $-1 \cdot 10^{-5}$ [°] | $-2 \cdot 10^{-5}$ [°] | $-3 \cdot 10^{-6}$ [°] |

The maximum payload masses that can be placed into the desired orbits obtained with the method presented in this paper compared to the reference data are shown in Figure 5. The mean absolute error of the data obtained with the proposed model is 5.5%. For 3 out of the 5 studied cases superior values for the payload mass have been found.

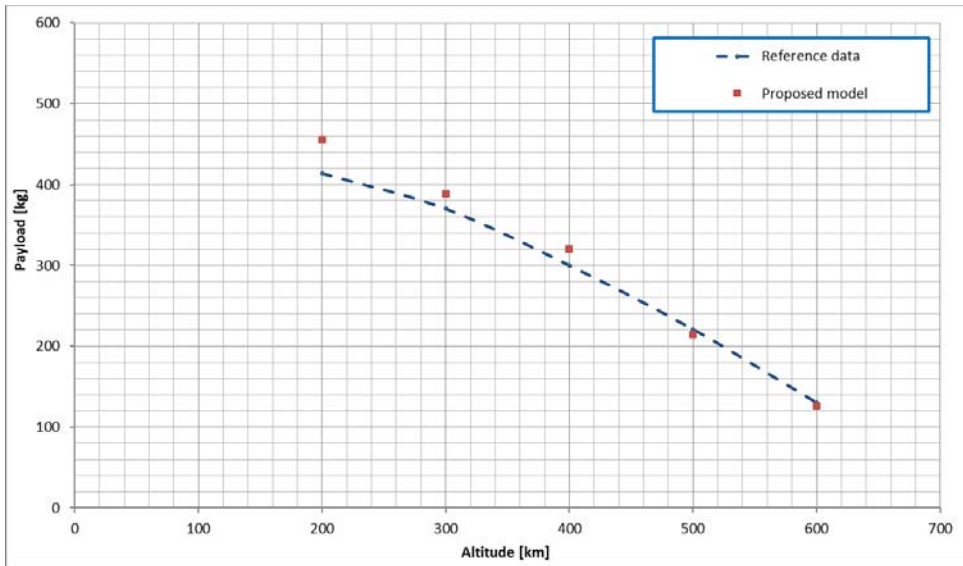


Figure 5 – Results, maximum payload mass, $i = 9.1^\circ$

Solution convergence was obtained after at least 100.000 iterations, the fastest being obtained for the 400 km altitude orbit (114.000 iterations). For the 400 km orbit, the code run time was approximately 5 hours. For this case, the objective function minimum value was found to be $f_{objective} = 0.9388$, corresponding to an orbit performance index $I_{orbit} = 0.0006$ and a constraints index $I_{constraints} = 1$ (all constraints have been respected). The 5 nominal trajectories computed for the 5 test cases are now shown together: altitude vs. time is shown in Figure 6, eccentricity vs. time is shown in Figure 7, climb angle vs. time is shown in Figure 8 and inclination vs. time is shown in Figure 9. These figures contain both the nominal launcher mission (solid lines) and the first 5 minutes of payload orbit (dotted lines).

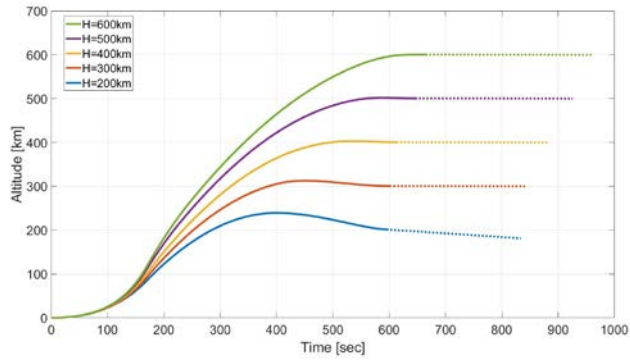


Figure 6 – Results, altitude vs. time

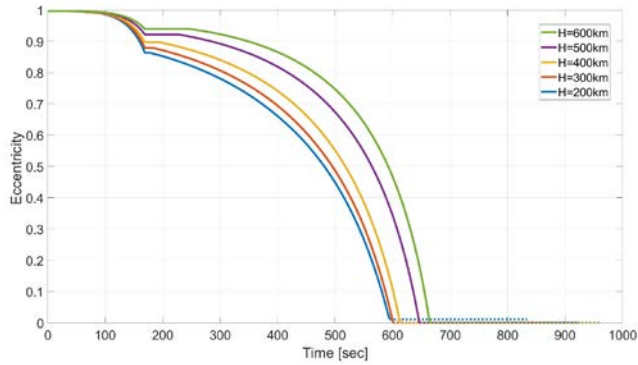


Figure 7 – Results, eccentricity vs. time

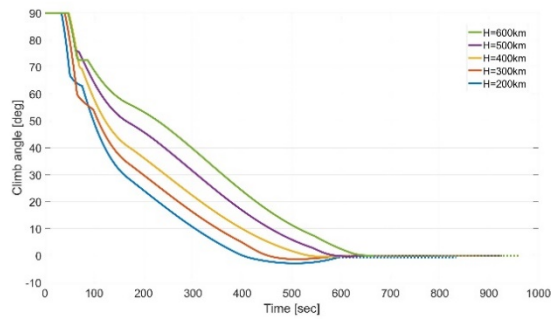


Figure 8 – Results, climb angle vs. time

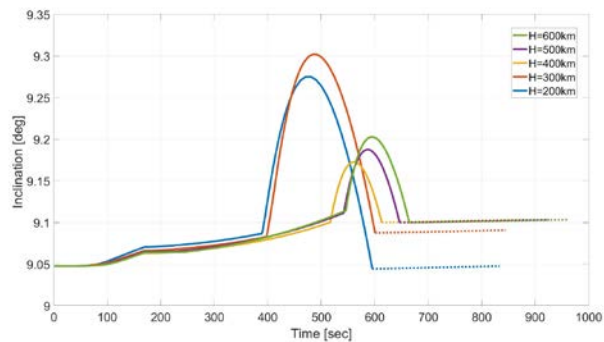


Figure 9 – Results, inclination vs. time

A more detailed view is now provided for the 400km altitude mission. Figure 10 presents the nominal trajectory of the launcher from launch (T0) until payload insertion (Ti). Figure 11 presents the nominal trajectory together with the first 5 minutes of payload orbit. Figure 12 presents the nominal trajectory together with the first 1.5 hours of payload orbit (almost 1 period). Finally, Figure 13 presents the first 24 hours after payload separation.

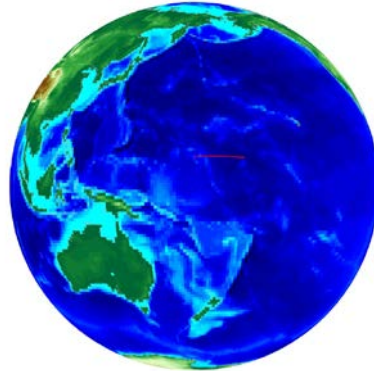


Figure 10 – Mercator projection 2D and Globe 3D views, Falcon 1 T0 – Ti

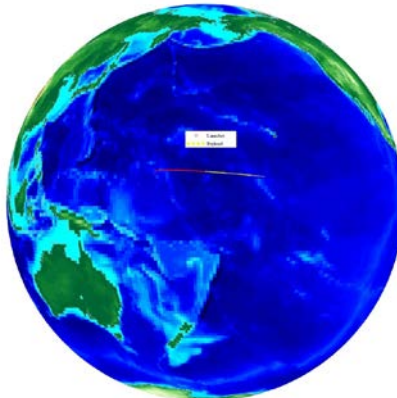
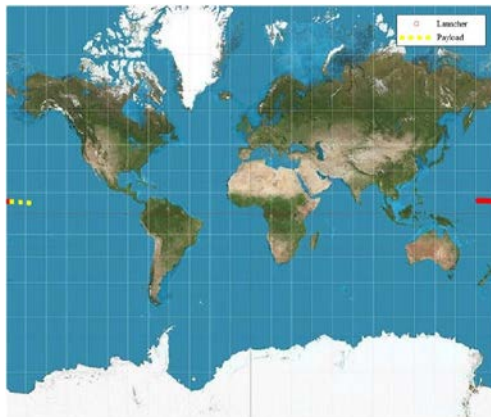


Figure 11 – Mercator projection 2D and Globe 3D views, Falcon 1 T0 – Ti+5min

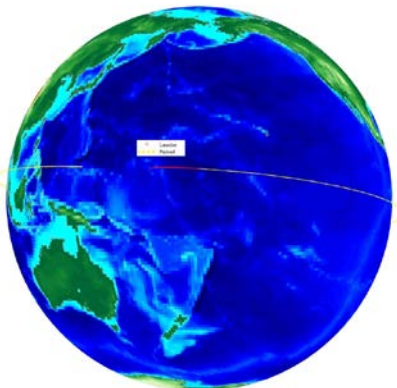


Figure 12 – Mercator projection 2D and Globe 3D views, Falcon 1 T0 – Ti+1.5h

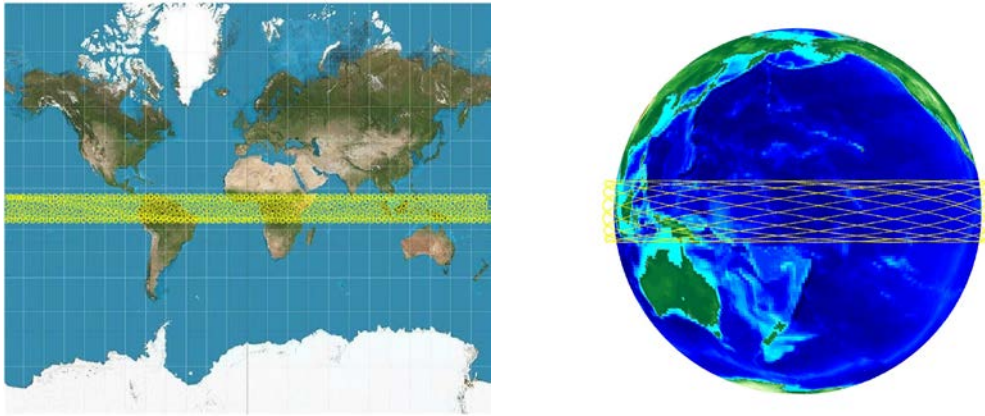


Figure 13 – Mercator projection 2D and Globe 3D views, Falcon 1 Ti – Ti+24h

7. CONCLUSIONS

The paper continues the work previous done in [1], [2], [3] extending the capabilities of a multidisciplinary optimisation tool for small launchers design. Mathematical models for trajectory assessment and optimisation are presented, results being validated with the aid of Falcon 1 reference data. A 3DOF dynamic model with null bank angle has been used, together with a feedback control scheme for climb angle and path track angle active guidance. The mean absolute error found was 5.5%, a higher payload mass being found in 3 out of the 5 test cases analysed [13].

REFERENCES

- [1] A. I. Onel, T. P. Afilipoae, A. M. Neculăescu, M. V. Pricop, MDO approach for a two-stage microlauncher, *INCAS Bulletin*, ISSN 2247–4528, vol. **10**, issue 3, pp. 127-138, 2018.
- [2] A. I. Onel, T. P. Afilipoae, A. M. Neculăescu, M. V. Pricop, Drag coefficient modelling in the context of small launcher optimisation, *INCAS Bulletin*, ISSN 2247–4528, vol. **10**, issue 4, pp. 103-116, 2018.
- [3] A. I. Onel, O. I. Popescu, A. M. Neculăescu, T. P. Afilipoae, T. V. Chelaru, Liquid rocket engine performance assessment in the context of small launcher optimisation, *INCAS Bulletin*, ISSN 2247–4528, vol. **11**, issue 3, pp. 135-145, 2019.
- [4] T. V. Chelaru and C. Mihăilescu, *Lansatoare si sisteme de lansare - Note de curs*, București: Editura Politehnica Press, 2017.
- [5] T. P. Afilipoae, A. M. Neculăescu, A. I. Onel, M. V. Pricop, A. Marin, A. G. Perșinaru, A. M. Cișmilianu, I. C. Oncescu, A. Toader, A. Sirbi, S. Bennani, T. V. Chelaru, Launch Vehicle - MDO in the development of a Microlauncher, *Transportation Research Procedia*, vol. **29**, pp. 1-11, 2018.
- [6] T. V. Chelaru, *Dinamica zborului – Îndrumar de proiect*, Ed. Politehnica Press, București, 2013.
- [7] A. A. Lebedev, N. F. Gerasiota, *Balistika raket*, Ed. Mașinostroenie, Moskva, 1970.
- [8] T. V. Chelaru, A. I. Onel, T. P. Afilipoae, A. M. Neculăescu, Mathematical model for microlauncher, performances evaluation, *U.P.B. Scientific Bulletin*, Series D, vol. **79**, issue 4, 2017.
- [9] T. V. Chelaru, C. Barbu, A. Chelaru, *Mathematical model in quasi-velocity frame for small launcher, technical solutions*, RAST 2015 - Proceedings of 7th International Conference on Recent Advances in Space Technologies 7208415, pp. 605-610.
- [10] T. V. Chelaru, A. Chelaru, A. I. Onel, Small Orbital Launcher Risk Zone Evaluation, *Incas Bulletin*, vol. **7**, nr. 3, 2015.
- [11] M. M. Peet, *Spacecraft Dynamics and Control*, Arizona State University, 2019.
- [12] T. V. Chelaru, A. I. Onel and A. Chelaru, Microlauncher, mathematical model for orbital Injection, *International Journal of Geology*, vol. **10**, 2016.
- [13] A. I. Onel, T. V. Chelaru, Aerodynamic assessment of axisymmetric launchers in the context of multidisciplinary optimisation, *INCAS Bulletin*, ISSN 2247–4528, vol. **12**, issue 1, 2020.

-
- [14] * * * SpaceX, *Falcon 1 Launch Vehicle Payload Users's Guide*, rev.7, 2008.
- [15] * * * *Space Launch Report: SpaceX Falcon Data Sheet*, <https://www.spacelaunchreport.com/falcon.html>.
- [16] * * * NASA Spaceflight, *New Falcon 1 type LV*, <https://forum.nasaspaceflight.com/>
- [17] G. Pezzella, A. Viviani, *Aerodynamic and aerothermodynamic analysis of space mission vehicles*, Springer, Switzerland, 2015.
- [18] A. I. Onel, A. Stavarescu, M. G. Cojocaru, M. V. Pricop, M. L. Niculescu, A. M. Neculaescu, T. P. Afilipoe, Computation of the Hypersonic Heat Flux with Application to Small Launchers, *AIP Conference Proceedings*, Volume **2046**, Issue **1**, 2018.
- [19] * * * A. Rohatgi, *Web based tool to extract data from plots, images and maps*, WebPlotDigitizer, Version: 4.2, San Francisco, USA, Available at <https://automeris.io/WebPlotDigitizer>.